Jurnal Polimesin
Department of Mechanical Engineering
State Polytechnic of Lhokseumawe
http://e-jurnal.pnl.ac.id/polimesin
e-ISSN : 2549-1999 No. : 2 Month : April
p-ISSN : 1693-5462 Volume : 23 Year : 2025

Processed dates: received on 2025-02-26, reviewed on 2025-03-27, accepted on 2025-04-23 and online availability on 2025-04-30

Impact of angle cap and water-filled blade modification on the output of overshot waterwheels

Rizki Afif Afandi, Dan Mugisidi*, Giri Parwatmoko, Oktarina Heriyani
Department of Mechanical Engineering, University of Muhammadiyah Prof. Dr. Hamka, Jakarta 13830, Indonesia
*Corresponding Author: dan.mugisidi@uhamka.ac.id

Abstract

The utilization of water resources as renewable energy through waterwheels presents an environmentally friendly alternative, however, its efficiency requires improvement through technological modification. This research investigates two design modifications: a 45° Angle Cap (AC) and a Water-Filled Angle Cap (WFAC), in comparison with a waterwheel without a Cap (WC). Experiments were conducted at discharges from 1 to 10 m³/h with a constant torque load of 0.05 N-m. The highest efficiency of 57.08% was achieved in the AC 45° configuration at 1 m³/h, generating 1.09 watts of power, while the WFAC 45° yielded the highest power output of 2.88 watts at 10 m³/h with an efficiency of 14.50%. Although increasing discharge generally led to higher power input, it was accompanied by a decrease in efficiency across all configurations. Among all three variations, WFAC 45° demonstrated superior performance at higher discharges, indicating its potential for enhancing the power and efficiency of overshot waterwheels.

Keywords:
Waterwheel, renewable energy, rotational kinetic energy, moment of inertia, efficiency.

1 Introduction

Sustainable utilization of natural resources is one of the central issues in the global effort to deal with climate change and environmental degradation [1], [2], including Indonesia. Indonesia is one of the developing countries that has abundant renewable natural resources and one of them is water [3]. Water as a renewable natural energy has great potential to be converted from kinetic energy into electrical energy [4]. Hydropower plants are designed to generate electricity on a large scale, while small-scale plants are known as Micro-hydro Power Plants (MHP) [5], [6], [7]. MHP utilizes the flow of rivers or other water sources to generate electricity in a sustainable manner to meet the needs of housing, agriculture, and community facilities [8], [9], [10].

The utilization of water as a renewable energy source requires a waterwheel that plays an important role in converting kinetic energy from water flow into other forms of energy and is usually converted into electrical energy through a generator that operates without reducing the volume of water [11], [12]. In this context, waterwheels were chosen because they are more environmentally friendly and cost-effective [13]. Waterwheels have 3 types: overshot, breast shot, and undershot waterwheels. [14]. In an overshot waterwheel, water flows from the top of the wheel and spins as it falls to a lower surface. In a breast shot waterwheel, water flows over the center of the waterwheel which is positioned parallel to the top [15]. Meanwhile, in an undershot waterwheel, the waterwheel is placed slightly above the water flow so that only the bottom part of the waterwheel enters the water. The difference between the three types of waterwheels lies in the type of energy transferred to the waterwheel which affects the efficiency and the exact conditions of use of each waterwheel. [16], [17].

Various studies have been conducted on waterwheels, including the effect of adding angled caps, blade thickness on flat-bladed waterwheels, and the relationship between blade height and power and efficiency [18], [19]. The efficiency of waterwheels is influenced by a variety of factors, including aspects of the geometry of the wheel, such as diameter size, number of blades, and their curved shape, as well as operational factors such as water level (head), flow discharge, load torque, and water flow position [20], [21]. To achieve high efficiency, more in-depth research is needed related to these factors, with experimental methods under field conditions [22]. Previous research shows that the shape of the waterwheel blades is very important because a certain shape makes it easier for water to enter between the blades and is one of the causes of the wheel's rotation. In addition, the moment of inertia of the waterwheel is also an important factor that affects the efficiency and stability of the waterwheel [23]. Although research on waterwheels has been going on for a long time, until now no waterwheel has been equipped with a director to force water to enter between the blades, even though this has the potential to increase the power generated. Another attempt that has not yet been made is to introduce water into the waterwheel to increase its moment of inertia.

Therefore, this study aims to determine the performance of the power generated by the wheel and the efficiency of the wheel's performance by comparing a straight-blade water wheel with a water wheel that has a blade cover to direct water in, as well as a wheel that contains water in the blade.

2 Method

The waterwheel used in the study is an overshot waterwheel with 16 blades. There are 2 models of blade caps, namely closed water-filled and 45° angled caps to the outside as shown in Fig. 1. The closed water-filled blades aim to produce a moment of inertia and increase the kinetic energy of the wheel. The cap that forms a 45° angle on the blades serves to expand the area outside the blades so that the water flow is concentrated in the blade area to achieve maximum rotation.

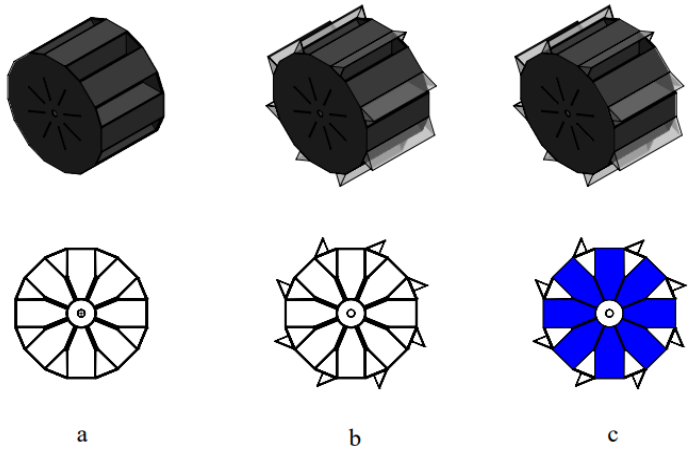

Fig. 1. Overshoot waterwheel. a) Isometric and side view Without Cap (WC), b) isometric and side view Angle Cap (AC) 45°, and c) isometric and side view Water-Filled Angle Cap (WFAC) 45°

The test method applied in the overshot waterwheel research is the actual experimental method on a laboratory scale. The test was carried out in the Mechanical Engineering laboratory of University Prof. Dr Hamka Muhammadiyah. Tests were carried out using dependent variables and independent variables. The dependent variable consists of rotation, torque, waterwheel power, and waterwheel efficiency. While the independent variables are Without Cap (WC), Angle Cap (AC) 45°, and Water-Filled Angle Cap (WFAC) 45° shown in Fig. 1. The flowchart of the overshot waterwheel research can be seen in Fig. 2.

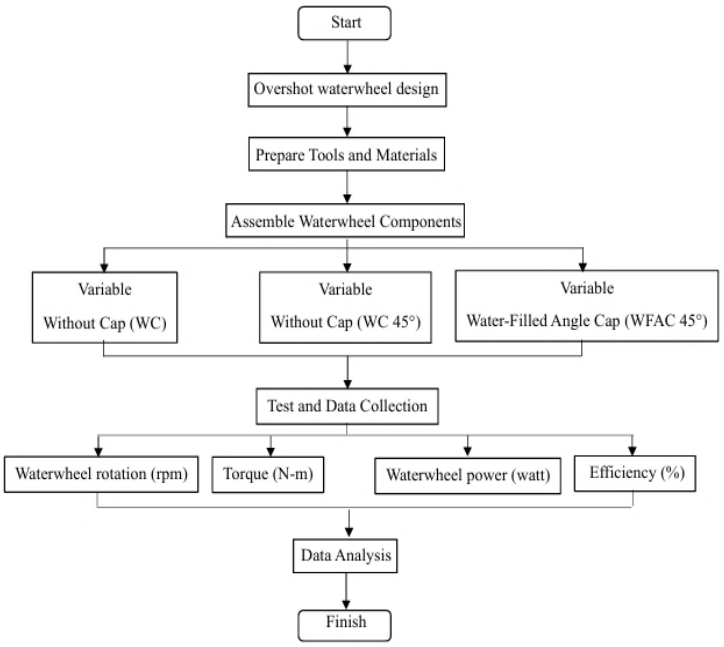

Fig. 2. Flowchart of overshot waterwheel research systematic

Fig. 2 is a systematic way of conducting overshot waterwheel research. This research consists of three interconnected stages. The first stage includes preparation of the design concept, equipment needed for research, and assembly of the waterwheel components. The second stage is a trial to ensure the research tool functions properly. The third stage is data collection through recording which is then followed by the data analysis process.

The design of the overshot waterwheel involved design, cutting, welding, and testing. The manufacture of the waterwheel housing uses melamine multiplex material, with the inside coated with resin and the outside coated with waterproof paint. The wheelhouse is 100 cm high, 100 cm long, and 37 cm wide. The lid is made of acrylic material with a 45° tilt angle. Meanwhile, the wheel is made of iron material with a thickness of 3 mm.

The wheel mounting frame plays a role in supporting the pillow block to support the wheel shaft, ensuring optimal wheel rotation. The waterwheel shaft is solid with a diameter of 25 mm, while the waterwheel has a diameter of 45 cm and a thickness of 30 cm. The geometry design of the overshot waterwheel in millimeters (mm) is shown in Fig. 3.

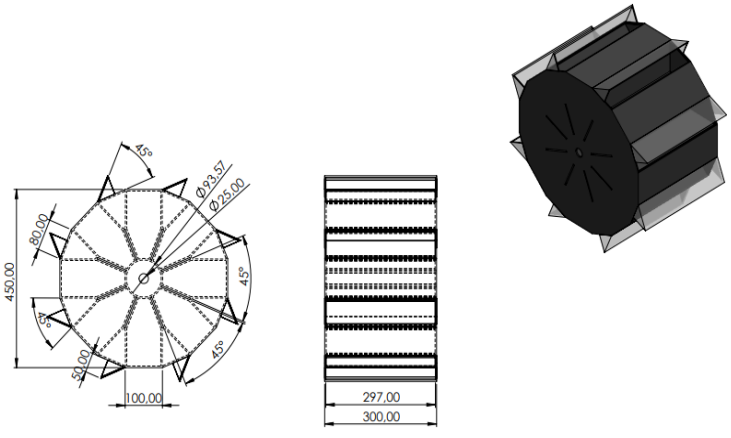

Fig. 3. Geometry of waterwheel

Measuring instruments used for the data collection process include, Torque meter functions to collect Torque data from the waterwheel. Data collection of waterwheel rotation using a Tachometer measuring instrument [24]. Water discharge settings using a Rotameter measuring instrument and water flow rate measured using a Flow velocity meter tool [25], according to the specifications listed in Table 1.

This study utilized one waterwheel to collect data on the independent variables. The four red-colored dots shown in the fig. 4 indicate the data collection locations required during the testing process.

Table 1. Specifications of waterwheel test measuring instrument

Measurement tool	Type	Capacity
Torque meter	Lutron TQ-8800	0 - 0.15 (N-m)
Tachometer	KW06-563	0 - 20.000 (rpm)
Rotameter	LZT-50S105/N	1 - 10 m^3 /h)
Flow velocity meter	Flo watch FL-03	2 - 150 (km/h)

Data was collected using flow rates of 1, 1.5, 2, 2.5, 3, 3.5, 4, 4.5, 5, 5.5, 6, 6.5, 7, 7.5, 8, 8.5, 9, 9.5, up to 10 m^3/h, which were circulated using a pump. The independent variables tested included a 45° angle cap, no cap, and a 45° angle cap with water content. Data was taken more than once to ensure the test results remained consistent.

The installation scheme of the overshot waterwheel test consists of 17 components, each of which plays a crucial role with different functions, starting from the water pump in charge of maintaining the continuity of water flow through the pipe from the waterwheel house, forwarded to the water trough according to the design shown in Fig. 4.

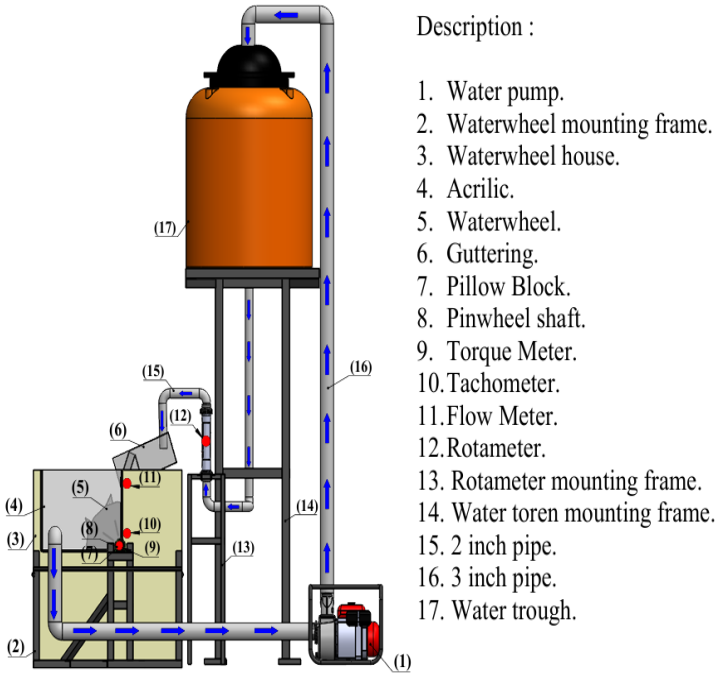

Fig. 4. Schematic design of overshot waterwheel testing installation

The water trough, which acts as the main reservoir, is designed to facilitate the precise regulation of water discharge, which is done with the help of a rotameter gauge to control the flow of water into the gutter. The gutter acts as a guide, concentrating the water flow precisely on the 45° tilt angle of the blades, ensuring an even distribution of water across the surface of the blades. The blade's main function is to maximize the efficiency of the waterwheel rotation by adjusting its rotation rate to the volume and velocity of the incoming water flow, which ultimately determines the overall performance of the waterwheel. As a control and reference in this test, the detailed specifications of the waterwheel are presented in Table 2, providing a clear guide to the technical parameters tested.

Table 2. Waterwheel specifications

Specification	Parameter
Weight of Waterwheel WC	41 kg
Weight of Waterwheel AC 45°	42.5 kg
Weight of Waterwheel WFAC 45°	60 kg
Toque	0.05 N-m

The precision-designed components of the waterwheel are then assembled into a highly complex and interconnected circuit, where each element contributes to the functionality of the entire system. The artificial waterways, whose continuity is supported by the use of pumps, serve to maintain a steady and controlled flow of water, which in turn allows for high-accuracy testing of the efficiency of the waterwheel. The overall result of the waterwheel assembly, which incorporates various aspects of technical design and construction, can be seen in Fig. 5.

Fig. 5. The assembled overshot waterwheel installation and data collection location. (a) water flow velocity data, (b) water discharge data, (c) waterwheel torque data, and (d) waterwheel rotation data

Experimental results were processed to determine the efficiency of the waterwheel. Energy from water can be obtained through water flowing into the blades of the waterwheel. The power generated by the water (P_{in}) can be calculated using Eq. (1) [26].

$$P_{in} = \rho . g . h . Q \quad (1)$$

Where P_{in} is water power (W), ρ is density of water (998.2 kg/m^3), g is gravitational acceleration (m/s^2), h is waterfall height (m), and Q is water discharge (m^3/h).

Where the head is the height difference between the surface of the base of the waterwheel housing and the height of the water surface before entering the waterwheel blades [27]. The circumferential speed of the wheel commonly known as angular velocity (ω) is obtained from Eq. (2) [28]. Meanwhile, to calculate the waterwheel power (P_{out}) using the Eq. (3) [29].

$$\omega = \frac{2 . \pi . n}{60} \quad (2)$$

$$P_{out} = T . \omega \quad (3)$$

Where ω is angular velocity (rad/s), n is waterwheel rotation (rpm), and T is torque (N-m).

The efficiency of the waterwheel (η) is the ratio between the power generated by the waterwheel and the water power, which can be calculated using Eq. (4) [30].

$$\eta = \frac{P_{out}}{P_{in}} \times 100\% \quad (4)$$

The rotation of a solid body with mass (m) moving translational (linear) with velocity (v) using Eq. (5) can be explained through kinetic energy according to Eq. (6) [31].

$$v = \omega . r \quad (5)$$

$$Ek = \frac{1}{2} . m . v^2 \quad (6)$$

Where r is distance of the waterwheel to the shaft (m), Ek is kinetic energy (J), m is mass of the wheel (kg), and v is water flow velocity (m/s^2).

It is assumed that the kinetic energy measured in a solid cylinder results in Rotational Kinetic Energy (Ek_{rot}) which is related to the moment of Inertia (I) and can be obtained through Eq. (7) [32].

$$Ek_{rot} = \frac{1}{2} . I . \omega^2 \quad (7)$$

Where is Ek_{rot} is rotational kinetic energy (J), and I is moment of inertia ($kg.m^2$).

Moment of Inertia (I) is the property of an object that allows it to maintain its position in rotational motion [33]. A stationary object tends to maintain its position, so a moving object will try to maintain its rotational motion. Mathematically, the moment of inertia can be obtained from Eq. (8).

$$I = m . r^2 \quad (8)$$

3 Results and discussion

After obtaining torque and rotation data for each discharge variation. Calculation of water power, waterwheel power, and overshot waterwheel efficiency using Eqs. (1), (3), and (4). The results of testing and data processing are presented in the form of tables and figures that show the relationship between these factors. The complete results of data processing can be seen in Table 3.

The rotation of the waterwheel is influenced by the water flow using Eq. (6) and the head of the waterwheel. At the discharge position of 1-5.5 m³/h, the head value was recorded at 0.7 m, while at the discharge of 6-8.5 m³/h, the head value increased by 0.02 m, and reached its peak at the discharge of 9 to 10 m³/h with a head value of 0.73 m. This increase in head is caused by the increase in water flow in the gutter of the waterwheel. The increase in head is caused by the increase in the flow of water flowing in the gutter of the waterwheel. The waterwheel without the corner cap experiences an obstacle, where the water flow cannot hit the entire blade optimally. As a result, the water flow that enters the blades is focused in the middle and goes straight down to the bottom of the wheel, so it cannot maximize the water flow and causes a small rotation.

On the other hand, the waterwheel with a 45° angle cap shows a larger rotation than the waterwheel without a cap, because the angle cap reduces the opening area of the waterwheel. This causes the flow of water into the blade of the waterwheel not to come out immediately, due to obstruction by the waterwheel cover, so that the water can be concentrated effectively towards the blade of the waterwheel.

Table 3. Data processing results of variable waterwheel WC, AC 45°, WFAC 45°

Q	n (rpm)			P_{in} (watt)			P_{out} (watt)			efficiency (%)		
(m^3/h)	WC	AC 45°	WFAC 45°	WC	AC 45°	WFAC 45°	WC	AC 45°	WFAC 45°	WC	AC 45°	WFAC 45°
1	7.41	19.62	8.95	1.91	1.91	1.91	0.41	1.09	0.51	21.70	57.08	26.55
1,5	11.96	25.66	18.31	2.86	2.86	2.86	0.66	1.43	1.07	23.21	50.09	37.53
2	16.22	30.02	19.91	3.82	3.82	3.82	0.89	1.70	1.21	23.30	44.50	31.69

Q	n (rpm)			P_{in} (watt)			P_{out} (watt)			efficiency (%)		
(m^3/h)	WC	AC 45°	WFAC 45°	WC	AC 45°	WFAC 45°	WC	AC 45°	WFAC 45°	WC	AC 45°	WFAC 45°
2,5	19.41	34.12	24.96	4.68	4.68	4.68	1.05	1.88	1.41	22.02	39.46	29.60
3	21.62	37.33	28.46	5.72	5.72	5.72	1.22	2.01	1.64	21.37	35.07	28.64
3,5	23.70	38.27	30.13	6.68	6.68	6.68	1.32	2.22	1.68	19.70	33.21	25.21
4	25.06	40.50	32.29	7.63	7.63	7.63	1.41	2.26	1.94	18.45	29.64	25.38
4,5	26.28	41.55	33.43	8.58	8.58	8.58	1.46	2.29	1.94	16.99	26.70	22.57
5	28.12	42.34	34.90	9.54	9.54	9.54	1.55	2.35	2.01	16.26	24.64	21.07
5,5	28.66	42.77	36.21	1049	10.49	10.49	1.56	2.42	2.01	14.88	23.05	19.16
6	29.75	43.38	37.39	11.77	11.77	11.77	1.66	2.36	2.23	14.11	20.07	18.96
6,5	31.95	43.96	38.42	12.75	12.75	12.75	1.74	2.30	2.21	13.64	18.05	17.35
7	33.11	44.13	39.06	13.73	13.73	13.73	1.80	2.43	2.32	13.13	17.72	16.88
7,5	34.20	45.06	39.67	14.72	14.72	14.72	1.91	2.52	2.20	12.98	17.10	14.96
8	36.04	45.86	40.58	15.70	15.70	15.70	1.95	2.67	2.35	12.42	17.03	14.98
8,5	36.68	46.51	41.68	16.68	16.68	16.68	2.09	2.63	2.37	12.52	15.77	14.22
9	38.99	46.87	42.59	17.90	17.90	17.90	2.14	2.60	2.51	11.94	14.53	14.03
9,5	39.91	47.30	44.73	18.90	18.90	18.90	2.24	2.68	2.58	11.87	14.15	13.63
10	41.47	48.56	47.47	19.89	19.89	19.89	2.29	2.85	2.88	11.50	14.32	14.50

Meanwhile, the wheel equipped with a corner cap filled with water experiences a moment of inertia that causes inertia in the rotation of the wheel to be smaller when the discharge is in the range of 1 to 4 m³/h. However, the rotation began to increase at a discharge of 4 to 10 m³/h due to the work of the moment of inertia helping to increase the kinetic energy of the waterwheel rotation, whereas, at a discharge of 10 m³/hour, the rotation of the waterwheel experienced a significant increase compared to the waterwheel using a 45° angle cap without water content. The following figure shows the comparison of the processed data.

Fig. 6 shows the relationship between water discharge (m³/h) on the horizontal axis and wheel speed (rpm) on the vertical axis. In this figure, there are three turbine configurations, namely AC 45°, WC, and WFAC 45°, with each tested at two water discharge ranges: 1-4 m³/h and 4-10 m³/h.

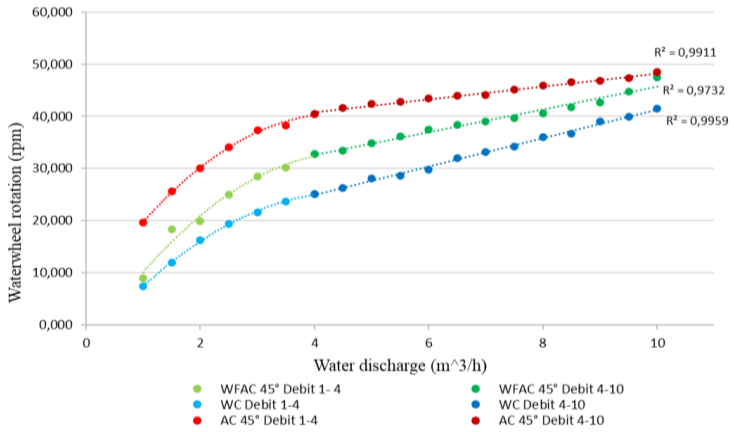

Fig. 6. Waterwheel rotation (rpm)

The AC 45° variable waterwheel represents a polynomial curve at small discharge (1-4 m^3/h), where the rotation of the waterwheel increases gradually from 19.62 rpm to 40.50 rpm. The increase in rotation is due to the angle cap which reduces the opening area of the waterwheel so that the water does not fall directly to the bottom of the waterwheel house, resulting in a moment of inertia with the calculation of Eq. (9) of 2.152 kg/m2 and generating rotational kinetic energy of 12.249 Joules using the calculation of Eq. (8). At large discharges (4-10 m³/h) show a more stable and linear increase, where the rotation of the waterwheel increases from 40.50 rpm to reach about 48.56 rpm. There is an increase in rotational kinetic energy of 23.386 Joules. The R^2 value is 0.9911, indicating that the 45° angle cap greatly influences the rotation of the waterwheel.

The WFAC 45° variable wheel represents a polynomial curve at small discharge, where the rotation of the wheel experiences inertia due to the water content of the wheel blades causing the rotation to slow down in contrast to the AC 45°. The rotation starts from about 8.95 rpm and increases to 32.29 rpm. In the increase in rotation, there is a moment of inertia of 3.087 kg/m^2 resulting in rotational kinetic energy of 9.242 Joules, with a slower increase when compared to the AC 45° waterwheel. At large discharge, the rotation of the waterwheel increased linearly from 32.29 rpm to 47.47 rpm showing a stable relationship between water discharge and waterwheel rotation. The curve also has a high fit to the data, indicated by the R^2 value of 0.9732. In the no-water-fill condition, with the same water discharge of 9-10 m³/h, the rotation of the waterwheel recorded a continuous increase, which was 46.87 rpm, 47.30 rpm, and 48.56 rpm. A significant increase in the rotation of the WFAC 45° began to be seen at a discharge of 9-10 m³/hour, respectively 42.59 rpm, 44.73 rpm, and 47.47 rpm and produced rotational kinetic energy of 25.946 Joules. Where water filling produces an increase in rotational kinetic energy, it causes a significant increase in wheel rotation. If the discharge continues the possibility is greater than with AC 45° which increases continuously. This is because the rotational kinetic energy is directly proportional to the square of the rotation speed at large discharge, although the difference in rotation is still visible.

The WC variable wheel showed a polynomial curve configuration at small discharge, with the wheel rotation starting from about 7.41 rpm and increasing up to 25.06 rpm. The moment of inertia value of 2.076 kg/m^2 produced 3.653 Joules less rotational kinetic energy compared to AC 45° and WFAC 45°, but still had a very high R^2 value of 0.9959 indicating an excellent match with the data. As the discharge was increased, the wheel rotation was only able to increase from 25.06 rpm to 41.47 rpm resulting in rotational kinetic energy of 12.470 Joules less than AC 45° and WFAC 45°, following a similar linear pattern as the other configurations. Overall, this figure shows that an increase in water discharge is closely related to an increase in waterwheel rotation just as in previous studies [34]. The difference in efficiency varies between wheel configurations and water discharge ranges.

Fig. 7 shows the relationship between water discharge (m³/h) and waterwheel power (watt), indicating that the higher the water discharge, the more power the waterwheel produces. This graph consists of several sets of data, each representing different conditions, namely AC 45°, WC, and WFAC 45° at discharge ranges of 1-4 m³/h and 4-10 m³/h, respectively. The difference between the small discharge range (1-4) and the large discharge range (4-10) can be seen from the different shapes of the curves used: polynomial curves for discharge 1-4 m^3/h and linear curves for discharge 4-10 m^3/h.

In the variable AC 45° waterwheel, the waterwheel configuration is at a 45° angle. In the discharge range of 1-4 m³/h, the curve shows a polynomial pattern, where the waterwheel power increases sharply from about 1.09 to almost 2.26 watts. In the discharge range of 4-10 m³/hr, the pattern changes to linear, with the power continuing to increase steadily until it reaches 2.85 watts at a discharge of 10 m³/hr. The R^2 = 0.8603 value for this linear curve indicates that the model does a good job of explaining the relationship between water discharge and waterwheel power.

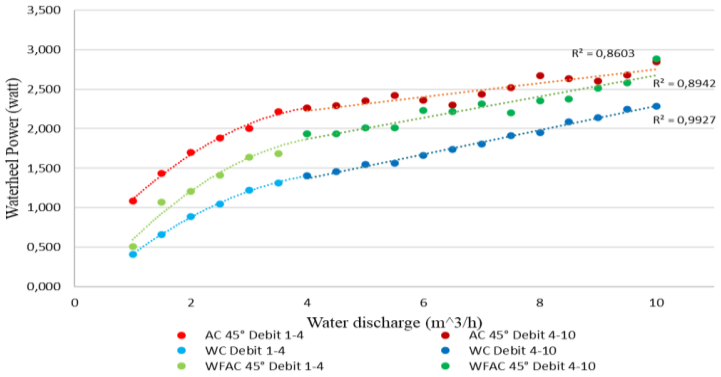

Fig. 7. Waterwheel power (Watt)

The WFAC 45° variable wheel, where at a discharge of 1-4 m³/h, the curve shows polynomial properties with the resulting wheel power relatively smaller than that of the AC 45°, which ranges from 0.51 watts to 1.94 watts. This phenomenon can be explained by the process of inertia caused by water, which makes the wheel heavier to rotate. So that the power generated is smaller than that of AC 45°. When the discharge increases from 4 to 10 m³/hour, the power of the waterwheel increases linearly until it reaches about 2.88 watts greater than AC 45°. This occurs because the increase in water discharge causes an increase in the moment of inertia, which in turn generates greater rotational kinetic energy, allowing the waterwheel power to reach its maximum point. The value of $R^2 = 0.8942$ for this linear curve indicates that the relationship between water discharge and waterwheel power is stronger than AC 45° at large discharge.

At the discharge range of 1-4 m³/h, the polynomial curve shows the generated waterwheel power starts from about 0.41 watts and increases up to 1.41 watts. In the discharge range of 4-10 m³/h, the waterwheel power increased linearly from 1.41 watts to 2.29 watts with a very strong relationship $R^2 = 0.9927$.

Fig. 8 illustrates the maximum and minimum waterwheel performance conditions observed in the operating system. The highest efficiency, recorded at variable AC 45°, occurred at a discharge of 1 m³/h, with an efficiency of 57.08%. In contrast, the lowest efficiency occurred at a discharge of 10 m³/h, with an efficiency of 14.32%. At variable WFAC 45°, the highest efficiency was achieved at a discharge of 1½ m³/h, which resulted in an efficiency of 37.53%.

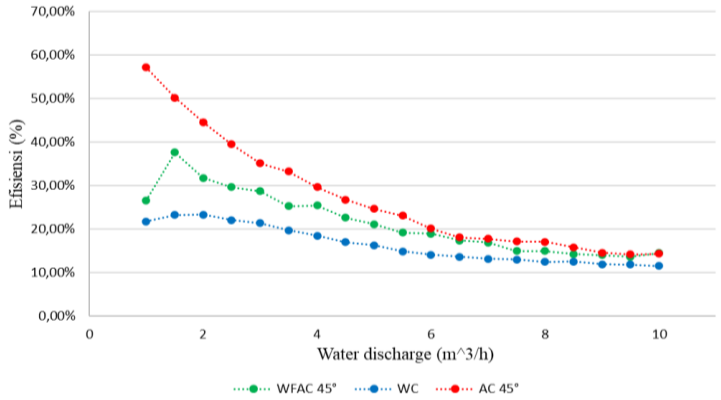

Fig. 8. Waterwheel efficiency (%)

An important phenomenon occurred at a discharge of 1 m³/h, where the efficiency initially decreased but then increased rapidly at a discharge of 1½ m³/h. This phenomenon can be attributed to the rotational inertia at a discharge of 1 m³/h, which causes the rotation of the waterwheel to rotate slowly. However, as the discharge increased, the water mass inside the waterwheel generated a moment of inertia similar to that observed in a previous study [35], which led to an increase in efficiency. The lowest efficiency at variable WFAC 45° was recorded at a discharge of 9½ m³/h, with a value of 13.63%. In addition, at a discharge of 2 m³/h, the maximum efficiency in the WC variable reached 23.30%, while the minimum efficiency at a discharge of 10 m³/h was 11.50%. Next, the efficiencies of the WC, AC 45°, and WFAC 45° compared to previous studies as shown in Table 4, in addition to the results of previous studies.

Table 4. Comparison of waterwheel performance efficiency with previous studies

Variable overshot water wheel	Efficiency	Reference
Waterwheel WC diameter 0.45 m	23.30%	
Waterwheel AC 45° diameter 0.45 m	57.08%	
Waterwheel WFAC 45° diameter 0.45 m	37.53%	
Waterwheel nozzle angle 30° diameter 0.50 m	25.05%	[36]
Waterwheel using square penstock diameter 0.60 m	42.00%	[37]
Waterwheel bucket configuration -20 diameter 0.90 m	45.00%	[38]

Based on Table 4, the efficiency of an overshot waterwheel is influenced by the blade design and the water flow system. The uncovered waterwheel (WC) was only able to achieve an efficiency of 23.30%. However, the use of a blade cover with a 45° angle (AC 45°) increased the efficiency to 57.08%. When water was introduced into the closed angle (WFAC 45°), the efficiency decreased to 37.53%, possibly due to water content in the closed blade. The use of a nozzle with a 30° angle resulted in an efficiency of 25.05%, which is still lower than the (WFAC 45°) configuration. The square-shaped penstock with a diameter of 0.60 m produced an efficiency of 42.00%, while the 0.90 m diameter bucket configuration showed an increase in efficiency to 45.00%, but still lower than the 0.45 m diameter 45° AC closed blade design. Overall, the closed blade design proved to be the most effective in improving efficiency compared to simply increasing the diameter.

4 Conclusion

The utilization of water resources as renewable energy through waterwheels presents an environmentally friendly alternative, however, its efficiency requires improvement through technological modification. This research investigates two design modifications: a 45° angle cap (AC) and a water-filled angle cap (WFAC), in comparison with a waterwheel without a cap (WC). Experiments were conducted at discharges from 1 to 10 m³/h with a constant torque load of 0.05 N-m. The highest efficiency of 57.08% was achieved in the AC 45° configuration at 1 m³/h, generating 1.09 watts of power, while the WFAC 45° yielded the highest power output of 2.88 watts at 10 m³/h with an efficiency of 14.50%. Although increasing discharge generally led to higher power input, it was accompanied by a decrease in efficiency across all configurations. Among all three variations, WFAC 45° demonstrated superior performance at higher discharges, indicating its potential for enhancing the power and efficiency of overshot waterwheels.

Acknowledgment

The authors express their sincere gratitude to the Renewable Energy Research Team, Faculty of Industrial Technology and Informatics, Universitas Muhammadiyah Prof. Dr. Hamka, for the financial support provided for this research.

References

[1] R. A. Febriansyar, T. Riyanto, dan I. Istadi, "Analysis of CaCO3 Impregnation on HY Zeolite Surface Area, Pore Size, and Activity in the Catalytic Cracking of Palm Oil to Biofuels," Teknik, vol. 43, no. 1, hal. 78–86, 2022, doi: 10.14710/teknik.v43i1.44579 Copyright.

[2] T. C. Lee, M. K. Anser, A. A. Nassani, M. Haffar, K. Zaman, dan M. M. Q. Abro, "Managing natural resources through sustainable environmental actions: A cross-sectional study of 138 countries," Sustain., vol. 13, no. 22, hal. 2–19, 2021.

[3] R. D. Syahrial, R. Soenoko, T. D. Widodo, dan A. Sunarso, "Pengaruh Tinggi Celah Aliran Pada Sluice Gate Terhadap Kinerja Kincir Air Jenis Sudu Melengkung," J. Rekayasa Mesin, vol. 14, no. 1, hal. 97–103, 2023.

[4] D. Mugisidi, I. N. Fauzi, O. Heriyani, Y. Djeli, E. Aidhilhan,

dan P. H. Gunawan, “Development of the Dethridge Wheel Blade Shape for Hydropower Generation in Irrigation Canals in Indonesia,” J. Adv. Res. Fluid Mech. Therm. Sci., vol. 98, no. 2, hal. 146–156, 2022.
[5] Y. D. Herlambang, G. Suwoto, B. M. Hermawan, F. G. Sumarno, P. Negeri, dan P. N. Semarang, “Micro Hydro Power Plant (MHP) performance using breast-shot waterwheel with different electrical load to improve efficiency,” Disseminating Inf. Res. Mech. Eng. Polimesin, vol. 22, no. 3, hal. 278–283, 2024.
[6] L. N. Rahayu dan J. Windarta, “Tinjauan Potensi dan Kebijakan Pengembangan PLTA dan PLTMH di Indonesia,” J. Energi Baru dan Terbarukan, vol. 3, no. 2, hal. 88–98, 2022.
[7] A. Rahman Hafiz, A. Nuramal, dan N. Iman Supardi, “Analisi Produksi Listrik di Pembangkit Listrik Tenaga Minihidro (PLTM) Analysis of Electricity Production in Mini Hydro Power Plants (PLTM),” Rekayasa Mek., vol. 6, no. 1, hal. 15–21, 2022.
[8] Y. Dewantoro Herlambang, G. Suwoto, B. Mei Hermawan, dan F. Gatot Sumarno, “The effect of variations in electric load on the performance of a 3 kW Micro Hydro Power Plant using an undershot waterwheel,” Disseminating Inf. Res. Mech. Eng. Polimesin, vol. 21, no. 2, hal. 214–218, 2023.
[9] R. Dyaa Sudiro, L. Halim, dan B. Made Arthaya, “Implementasi Dan Pengujian Prototipe Turbin Jenis Propeller Untuk Pembangkit Listrik Tenaga Mikrohidro,” J. Rekayasa Mesin, vol. 15, no. 2, hal. 919–936, 2024.
[10] E. Quaranta dan R. Revelli, “Gravity water wheels as a micro hydropower energy source: A review based on historic data, design methods, efficiencies and modern optimizations,” Renew. Sustain. Energy Rev., vol. 97, hal. 414–427, 2018.
[11] M. H. Kurniawan, A. Eksperimental, P. Performa…, dan K. K. Ayuningtiyas, “Analisis Eksperimental Pengaruh Performa Aliran Natural (Tanpa Pengarah) dan Penggunaan Nozzle Pada Kincir Air Jenis Breastshot,” Indones. J. Eng. Technol., vol. 5, no. 1, hal. 2623–2464, 2022.
[12] K.-L. Weng, F.-C. C. Chen, dan Y.-H. Lee, “Application Of Water Energy System To Balance Energy And Environment In The Whole World,” IEEE Eurasia Conf. IOT,Communication Eng., hal. 21–23, 2019.
[13] E. Quaranta dan R. Revelli, “Performance Optimization of Overshot Water Wheels at High Rotational Speeds for Hydropower Applications,” J. Hydraul. Eng., vol. 146, no. 9, hal. 1–5, 2020.
[14] A. Agato, A. sunarso Sunarso, N. Narsih, D. S. Domi, dan D. Iswanda, “Optimasi Unjuk Kerja Kincir Air Undershot,” J. Rekayasa Mesin, vol. 14, no. 1, hal. 251–260, 2023.
[15] H. Putra Prabawa, D. Mugisidi, M. Yusuf D, dan O. Heriyani, “Pengaruh Variasi Ukuran Diameter Nozzle Terhadap Daya Dan Efisiensi Kincir Air Sudu Datar,” in Jurnal UMJ, 2016, hal. 1–8.
[16] Warjito, D. Adanta, Budiarso, dan A. P. Prakoso, “The effect of bucketnumber on breastshot waterwheel performance,” in IOP Conference Series: Earth and Environmental Science, Jan 2018, hal. 1–7.
[17] F. J. Sánchez-Jiménez dan J. A. González, “Watermills: The origin of the use of renewable hydraulic energy in Spain,” Ind. Archaeol. Rev., vol. 40, no. 1, hal. 2–10, 2018.
[18] I. Gunawan Widodo, A. Sunarso, H. Sihombing, dan D. Sulistiono, “Pengaruh Kedalaman Pencelupan Sudu Kincir Terhadap Unjuk Kerja Kincir Air,” J.Rekayasa Mesin, vol. 13, no. 2, hal. 62–66, 2018.
[19] M. H. Nguyen, H. Jeong, dan C. Yang, “A study on flow fields and performance of water wheel turbine using experimental and numerical analyses,” Sci. China Technol. Sci., vol. 61, no. 3, hal. 464–474, 2018.
[20] E. Quaranta dan R. Revelli, “Hydraulic Behavior and Performance of Breastshot Water Wheels for Different Numbers of Blades,” J. Hydraul. Eng., vol. 143, no. 1, hal. 1–10, Jan 2017.
[21] D. Mugisidi, O. Heriyani, R. A. Luhung, dan M. R. D. Andrian, “Utilization of the dethridge wheel as a low head power generator and loss analysis,” in MATEC Web of Conferences, 2018, hal. 1–6.
[22] Agato, Deendarlianto, Indarto, dan A. Sunarso, “Simulasi Numerik Aliran Fluida Pada Kincir Air Menggunakan Metode Sliding Mesh Interface,” J. Rekayasa Mesin, vol. 15, no. 2, hal. 955–966, 2023.
[23] M. Castro-García, J. I. Rojas-Sola, dan E. De La Morena-de La Fuente, “Technical and functional analysis of Albolafia waterwheel (Cordoba, Spain): 3D modeling, computational-fluid dynamics simulation and finite-element analysis,” Energy Convers. Manag., vol. 92, hal. 207–214, 2015, doi: 10.1016/j.enconman.2014.12.047.
[24] S. D. Boedi, A. N. Mekel, dan A. Maidangkay, “Rancang Bangun Turbin Kinetik Sudu Berengsel Luar Sebagai Pembangkit Listrik Skala Pikohidro,” Otopro, vol. 17, no. 2, hal. 69–75, 2022.
[25] N. Mandal dan G. Rajita, “An accurate technique of measurement of flow rate using rotameter as a primary sensor and an improved op-amp based network,” Flow Meas. Instrum., vol. 58, hal. 38–45, 2017.
[26] M. R. Ramdhani, R. Irwansyah, Budiarso, Warjito, dan D. Adanta, “Investigation of the 16 blades pico scale breastshot waterwheel performance in actual river condition,” J. Adv. Res. Fluid Mech. Therm. Sci., vol. 75, no. 1, hal. 38–47, 2020.
[27] J. Štigler, “Overshot water wheel efficiency measurements for low heads and low flowrates,” EPJ Web Conf., vol. 269, hal. 01058, 2022.
[28] M. F. Basar, I. A. Zulkarnain, K. Sopian, dan N. A. Mohd Rais, “Investigations on the performance of bottle blade overshot water wheel in very low head resources for pico hydropower,” Energy Harvest. Syst., vol. 11, no. 1, hal. 2–10, 2024.
[29] Z. Nurfadilah, D. Mugisidi, A. Rahman, S. Pohan, dan O. Heriyani, “Pengaruh Kincir Tertutup Terhadap Efisiensi dan Rugi-rugi,” Rekayasa Energi Manufaktur) J. |, vol. 8, no. 1, hal. 2528–3723, 2023.
[30] E. Quaranta dan R. Revelli, “Output power and power losses estimation for an overshot water wheel,” Renew. Energy, vol. 83, hal. 979–987, 2015.
[31] M. Darwis, “Analisis Pengaruh Pembukaan Katup Terhadap Kinerja Turbin Air,” J. P4I, vol. 3, no. 4, hal. 365–376, 2023.
[32] Marinus S, Hiendro A, dan Yandri, “Studi Aplikatif Roda Gila (FLYWHEEL) Pada Pembangkit Listrik Tenaga Mikrohidro (PLTMH),” J. Elektr. Eng. Energy Inf. Teknol., vol. 7, no. 1, hal. 1–9, 2019.
[33] A. Digdoyo, F. Rahmasari, A. Budi Djatmiko, E. Yuniaty, dan D. Saepul Anwar, “Rancang Bangun Alat Uji Momen Inersia Massa Suatu Elemen Mesin dalam Tiga Arah Sumbu,” J. Ilm. Rekayasa Dan Inov., vol. 4, no. 2, hal. 193–200, 2022.
[34] M. F. Basar, N. A. M. Rais, A. A. Rahman, W. A. Mustafa, K. Sopian, dan K. V. Wong, “Optimization of Reaction Typed Water Turbine in Very Low Head Water Resources for Pico Hydro,” J. Adv. Res. Fluid Mech. Therm. Sci., vol. 90, no. 1, hal. 23–39, 2022.
[35] D. Iswanda, R. Soenoko, W. Winarto, dan A. Sunarso, “Pengaruh Besar Sudut Butterfly Guide terhadap Unjuk Kerja Kincir Air,” J. Rekayasa Mesin, vol. 12, no. 3, hal. 653–661, Des 2021, doi: 10.21776/ub.jrm.2021.012.03.15.
[36] I. Wayan, B. Saputra, dan A. I. Weking, “Rancang Bangun Pemodelan Pembangkit Listrik Tenaga Mikro Hidro (PLTMH) Menggunakan Kincir Overshot Wheel,” Teknol. Elektro, vol. 16, no. 02, 2017.
[37] T. Harismandri, J. Teknik Mesin, F. Teknik Universitas Riau Kampus Binawidya Km, dan S. Baru Panam, “PENGUJIAN PRESTASI KINCIR AIR TIPE OVERSHOT DI IRIGASI

KAMPUS UNIVERSITAS RIAU DENGAN PENSTOCK BERVARIASI," 2017.
[38] J. Štigler, "Overshot water wheel efficiency measurements for low heads and low flowrates," EPJ Web Conf., vol. 269, hal. 01058, 2022.